Science of the Total Environment 598 (2017) 669–679

Contents lists available at ScienceDirect

Science of the Total Environment

journal homepage: www.elsevier.com/locate/scitotenv

Land cover change during a period of extensive landscape restoration in Ningxia Hui Autonomous Region, China

Angela M. Cadavid Restrepo [a,*], Yu Rong Yang [b,c], Nicholas A.S. Hamm [d], Darren J. Gray [a,c], Tamsin S. Barnes [e,f], Gail M. Williams [g], Ricardo J. Soares Magalhães [e,h], Donald P. McManus [c], Danhuai Guo [i], Archie C.A. Clements [a]

[a] Research School of Population Health, The Australian National University, Canberra, Australian Capital Territory 0200, Australia
[b] Ningxia Medical University, 692 Shengli St, Xingqing, Yinchuan, Ningxia Hui Autonomous Region, PR China
[c] Molecular Parasitology Laboratory, QIMR Berghofer Medical Research Institute, Brisbane, Queensland 4006, Australia
[d] Faculty of Geo-Information Science and Earth Observation (ITC), University of Twente, Hengelosestraat 99, 7514 AE Enschede, Netherlands
[e] School of Veterinary Science, The University of Queensland, Main Dr & Outer Ring Road, Gatton, Queensland 4343, Australia
[f] Queensland Alliance for Agriculture and Food Innovation, The University of Queensland, Gatton, Queensland 4343, Australia
[g] School of Public Health, The University of Queensland, Brisbane, Queensland 4006, Australia
[h] Children's Health and Environment Program, Queensland Children's Medical Research Institute, The University of Queensland, Brisbane, Queensland 4101, Australia
[i] Computer Network Information Center, Chinese Academy of Sciences, Haidian District, Beijing 100190, PR China

HIGHLIGHTS

- We found an increase in forest, herbaceous vegetation and in regenerating bareland.
- The largest relative change for the period 1991–2015 was observed in the area covered by forest.
- The increase in forest resulted mainly from conversion of cultivated land and herbaceous vegetation.
- Forest growth primarily occurred in the north and south of the province.

GRAPHICAL ABSTRACT

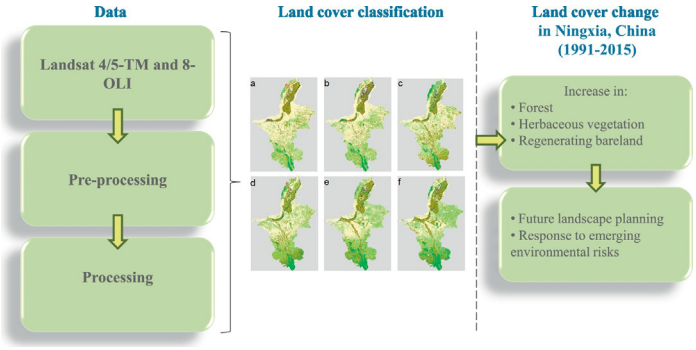

ARTICLE INFO

Article history:
Received 25 October 2016
Received in revised form 31 March 2017
Accepted 17 April 2017
Available online xxxx

Editor: Ouyang Wei

Keywords:
Environmental change
Land cover change
Geographic information systems

ABSTRACT

Environmental change has been a topic of great interest over the last century due to its potential impact on ecosystem services that are fundamental for sustainable development and human well-being. Here, we assess and quantify the spatial and temporal variation in land cover in Ningxia Hui Autonomous Region (NHAR), China. With high-resolution (30 m) imagery from Landsat 4/5-TM and 8-OLI for the entire region, land cover maps of the region were created to explore local land cover changes in a spatially explicit way. The results suggest that land cover changes observed in NHAR from 1991 to 2015 reflect the main goals of a national policy implemented there to recover degraded landscapes. Forest, herbaceous vegetation and cultivated land increased by approximately 410,200 ha, 708,600 ha and 164,300 ha, respectively. The largest relative land cover change over the entire study period was the increase in forestland. Forest growth resulted mainly from the conversion of herbaceous vegetation (53.8%) and cultivated land (30.8%). Accurate information on the local patterns of land cover in NHAR may contribute to the future establishment of better landscape policies for ecosystem management and

* Corresponding author at: Research School of Population Health, The Australian National University, Building 62 Mills Road, Canberra, Australian Capital Territory, Australia.
E-mail addresses: angela.cadavid@anu.edu.au (A.M. Cadavid Restrepo), Yurong.Yang@qimrberghofer.edu.au (Y.R. Yang), n.hamm@utwente.nl (N.A.S. Hamm), u5624503@uds.anu.edu.au (D.J. Gray), t.barnes@uq.edu.au (T.S. Barnes), g.williams@sph.uq.edu.au (G.M. Williams), r.magalhaes@uq.edu.au (R.J. Soares Magalhães), Don.McManus@qimrberghofer.edu.au (D.P. McManus), guodanhuai@cnic.cn (D. Guo), director.rsph@anu.edu.au (A.C.A. Clements).

http://dx.doi.org/10.1016/j.scitotenv.2017.04.124
0048-9697/

Remote sensing
Earth observations

protection. Spatially explicit information on land cover change may also help decision makers to understand and respond appropriately to emerging environmental risks for the local population.

1. Introduction

Changes in land use and land cover (LULC) are fundamental components of environmental change, and are major determinants of sustainable development and human adaptation to global change (Turner et al., 2007; Turner et al., 1993). Land cover (biophysical cover of the Earth's surface) and land use (description of how humans use the land) are of great significance in maintaining the structure and productivity of ecological systems (Lambin et al., 2001). LULC change influences the climate system through effects on the Earth's surface albedo (the fraction of incident electromagnetic radiation reflected by the land surface) and the exchange of greenhouse gases between the soil and the atmosphere (Foley et al., 2005; Pielke et al., 2002). Thus, land cover change has the potential to impact on climate change at local and regional scales (de Noblet-Ducoudré et al., 2012; Kalnay and Cai, 2003) and also at a global scale (Foley et al., 2005). Some extensive LULC changes may also contribute to diminish or accelerate soil erosion, homogenization of the agricultural landscape and subsequent loss or fragmentation of natural habitats (Blaikie and Brookfield, 2015; Bommarco et al., 2013). These effects have the potential to alter biodiversity (Newbold et al., 2015; Sala et al., 2000) to such an extent that the well-being and vulnerability of humans to social and environmental stressors may be positively or negatively affected (Carpenter et al., 2006).

Human population growth and economic expansion are widely recognised as major anthropogenic drivers of LULC change (Vitousek et al., 1997). Approximately one-third to one-half of the Earth's land surface has already been modified considerably by human activities (Vitousek et al., 1997), and the extent of this transformation may increase to compensate for the growing demand for food and natural resources (Bommarco et al., 2013). In response to the concerns about human capability to adapt to a changing environment, interdisciplinary assessments of LULC status and change have become increasingly important subjects of environmental change research (Verburg et al., 2009).

Since the start of economic reforms in China in 1978, the country has sustained accelerated economic growth and urban expansion. The total population grew from about 980 million people in 1980 to 1.36 billion people in 2013 (National Bureau of Statistics of China, 2014). Resultant social restructuring processes have led to an environmental transformation of unprecedented proportions (Liu and Diamond, 2005). Projects such as the Three-Gorges Dam across the Yangtze River, designed to promote infrastructure and economic development in the country, have been associated with alterations to biodiversity and ecosystem properties in several regions (Xu et al., 2013). To mitigate the adverse impacts of socio-economic and demographic changes, the Chinese government has responded by implementing a series of land reform policies and incentive programs to reduce land degradation and promote sustainable development in rural China (The University of Nottingham, 2010).

The Grain for Green Project (GGP), also called the Sloping Land Conversion Program, implemented since 2002 after a short pilot between 1999 and 2001, is the largest ecosystem service payment project in the country (Liu et al., 2008; Wang et al., 2007). Under the GGP, the government offers farmers annual grain and cash subsidies as well as free seeds or seedlings per area of converted land to reduce soil erosion (Yin and Yin, 2010). The project focuses primarily on the reduction of cropland on steep slopes by promoting three types of land conversions: cropland to forest, cropland to grassland, and sandy land that cannot be used for arable production to forest (The University of Nottingham, 2010; Zhou et al., 2012). The GGP also advocates for prohibition of enclosures for grazing, and sand storm prevention and control (Wang et al., 2007). Some of the immediate ecological benefits of the land restoration program include increased forest coverage, control of soil erosion, and reduced water surface runoff and spread of wind-blown dust (Fan et al., 2015). However, work is still required to explore the additional ecological, climatic and public health consequences that can result from the long-term implementation of the GGP and other similar environmental initiatives (Liu et al., 2008; Pielke, 2005). NHAR is a province located in arid and semi-arid areas across the Loess Plateau and the Yellow River plains which are priority regions for the implementation of the GGP (Liu et al., 2008; The University of Nottingham, 2010). The high local poverty rates, the difficult natural environmental conditions and the over-exploitation of natural resources in NHAR have contributed to the deterioration of the local ecological environment in past decades.

Earth observation (EO) data collected using satellite remote sensing and in situ observations, have been used extensively to characterize and monitor LULC change (Broich et al., 2014; Carreiras et al., 2014; Hamm et al., 2015; Shalaby and Tateishi, 2007; Turner et al., 2007; Yuan et al., 2005). Recently, the wide availability of very fine- (<10 m) and fine- (10 to 100 m) resolution imagery from satellite sensors such as Landsat, QuickBird and IKONOS, have provided new opportunities to represent more accurately LULC at finer spatial resolutions (J. Chen et al., 2015; Hamm et al., 2015; Raj et al., 2013; Sawaya et al., 2003). EO data and geographic information systems (GIS) have been applied in China to guide scientific activities that focus on the assessment and monitoring of the short- and long-term effects of different land use and management practices implemented at various administrative levels (Fan et al., 2015; Liu et al., 2014; Weng, 2002).

This study aims to quantify and describe the spatial and temporal patterns of land cover change in NHAR during a period of extensive landscape restoration. Maps that document accurately the local patterns of land cover change in this province can form the basis for future landscape planning and ecosystem management and protection. This spatially explicit information on land cover change may also help to understand and respond rapidly and effectively to emerging environmental risks such as natural disasters, infectious diseases and food insecurity for the local population.

2. Materials and methods

2.1. Study area

NHAR is a small province located on the upper reaches of the Yellow River in northwest China between latitudes 35°26′ N and 39°30′ N, and between longitudes 104°50′ E and 107°40′ E. NHAR shares borders with the Inner Mongolia Autonomous Region in the north, Gansu Province in the south and west and Shaanxi Province in the east. From north to south, the provincial territory stretches 465 km, and from east to west between 45 km and 250 km, with a total area is 66,400 km^2. NHAR consists of five prefectures that are subsequently subdivided into counties, townships and villages. By the end of 2014, the total population amounted to 6.6 million people of which 53.6% were living in urban areas and 46.4% in rural areas (Li et al., 2008; Statistical Bureau of Ningxia Hui Autonomous Region, 2014).

NHAR lies at ~1000 m above sea level. The territory is geographically diverse and consists of three major natural regions that have distinct agricultural production systems: the northern Yellow River Irrigated District (irrigated agricultural system), the central desertified district (a mix of rainfed and irrigated areas with extensive grazing) and the

southern mountainous and loess hilly district (with a rainfed agricultural system). These regions cover 23.7%, 45% and 31.3% of the NHAR territory, respectively (Li et al., 2008; Li et al., 2013). Elevation increases from north to south with the highest peak at 3556 m. In general, the province has a temperate continental monsoon climate and four distinct seasons. Temperature varies from 24 °C in July to −9 °C in January with an annual average of 9.5 °C. Rainfall varies from 180 to 800 mm year^{-1} increasing from north to south. Most rainfall occurs during the summer and autumn months (80% of the total precipitation in the entire region). The annual average rainfall is 289 mm year^{-1} (Li et al., 2008) (Fig. 1).

2.2. Environmental data

2.2.1. Remotely sensed data

The Landsat Surface Reflectance Climate Data Record (Landsat CDR) was the main source of the data used for land cover classification and change detection analyses. Landsat CDR data sets, also called Landsat level 2A products, are high-level data products that were generated by applying atmospheric correction routines to Landsat Level 1 scenes (Department of the Interior - The United States Geological Survey (USGS), 2016a; Department of the Interior - The United States Geological Survey (USGS), 2016b). The Landsat CDR uses the Universal Transverse Mercator (UTM) projection (48N for NHAR). For the study, time series of Landsat CDR data sets processed from Landsat 4–5 Thematic Mapper (Landsat 4–5 TM) and Landsat 8 Operational Land Imager and Thermal Infrared Sensor (Landsat-8 OLI/TIRS) were downloaded for the period 1990 to 2015 at five-year intervals. This time period was selected due to the increased availability of cloud-free data. Images were acquired from the Earth Explorer website (The United States Geological Survey (USGS)). For most years, four scenes were required to cover the entire territory. However, due to the presence of clouds in most of the available images from 1990 and 1995, Landsat data from the years 1991 and 1996 were obtained and used for classification (Table 1). Also for the years 1996 and 2000, a fifth scene was required to fill the missing data. The primary scene selection criteria were based on acquisition dates. To the extent possible, images were collected from the period June to November each year which corresponds to the summer and autumn growing seasons in NHAR. However, actual image acquisition dates varied depending on the availability of the data. When there were no scenes available for the selected months, the closest-in-time and most cloud-free scenes available were downloaded for the analyses (Table 1).

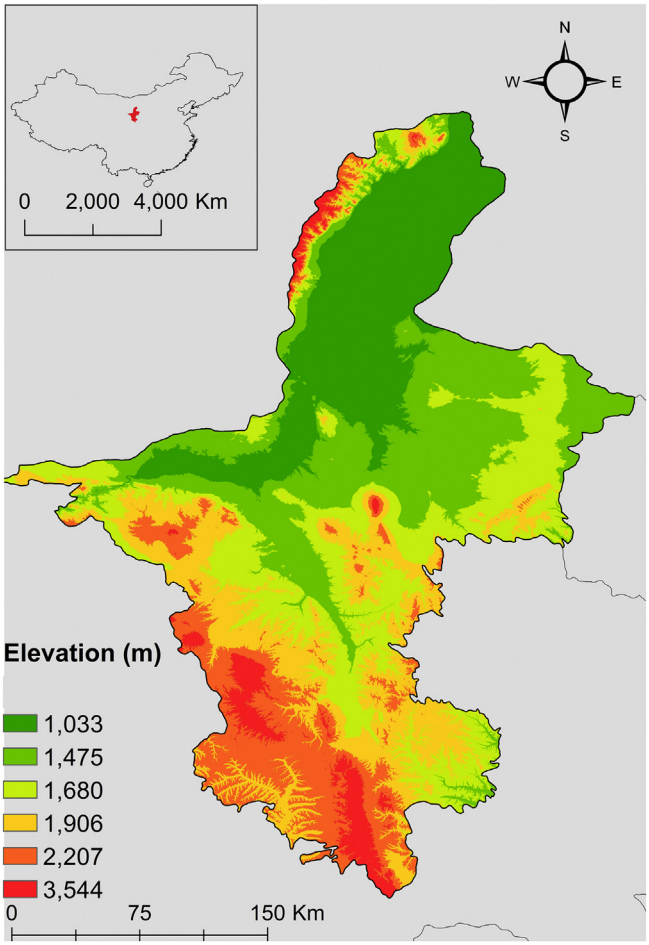

Fig. 1. Map and elevation of NHAR and location of the province within China (inset).

2.2.2. Elevation data

Topographic correction was performed to reduce terrain illumination effects on the retrieved data. To apply the topographic correction algorithm, information on solar position according to the acquisition time of the images, and on the slope and aspect of the terrain are required. Therefore, in addition to the Landsat metadata files, the Advanced Spaceborne Thermal Emission and Reflection Radiometer (ASTER) Global Digital Elevation Model (GDEM) version 2 was downloaded from the USGS Earth Explorer website (The National Aeronautics and Space Administration (NASA) and Ministry of Economy Trade and Industry (METI), 2011; The United States Geological Survey (USGS)). It was necessary to project the ASTER DEM to match the Landsat imagery. Using nearest-neighbour resampling, the GDEM data were projected to the Universal Transverse Mercator (UTM) coordinate system zone 48N and resampled to a 30 m spatial resolution using ArcGIS software version 10.3.1 (ESRI, 2015).

2.2.3. Reference data for image classification

Due to the lack of reference information on land cover information for NHAR during the study period, multiple data sources were required to produce reference data sets for land cover classification (training). Training data for the years 2000 and 2010 were obtained from random sampling of a combination of relatively fine-scale global maps, the GlobeLand30 and the global forest/non-forest maps (FNF) (Japan

Table 1
Specifications for the Landsat scenes used for land cover classification and change detection analyses in Ningxia Hui Autonomous Region from 1991 to 2015.

Year	Data type	Landsat scene	Path/row	Date acquired
1991	Landsat 4–5 Thematic Mapper	LT51290331989236BJC00	129/033	24/08/1989
		LT51290341991242BJC00	129/034	30/08/1991
		LT51290351991242BJC00	129/035	30/08/1991
		LT51300341993158CLT00	130/034	07/06/1993
1996	Landsat 4–5 Thematic Mapper	LT51290331995253CLT00	129/033	10/09/1995
		LT51290341996128CLT00	129/034	07/05/1996
		LT51290351996112CLT00	129/035	21/04/1996
		LT51300341996215BJC00	130/034	02/08/1996
		LT51300341996023CLT00	130/034	23/01/1996
2000	Landsat 4–5 Thematic Mapper	LT51290332000235BJC00	129/033	22/08/2000
		LT51290342000235BJC00	129/034	22/08/2000
		LT51290352001141BJC00	129/035	21/05/2001
		LT51300332000258BJC00	130/033	14/09/2000
		LT51300342000242BJC00	130/034	29/08/2000
2005	Landsat 4–5 Thematic Mapper	LT51290332005296BJC00	129/033	23/10/2005
		LT51290342005280BJC00	129/034	07/10/2005
		LT51290352005280BJC00	129/035	07/10/2005
		LT51300342005303BJC00	130/034	30/10/2005
2010	Landsat 4–5 Thematic Mapper	LT51290332010182IKR00	129/033	01/07/2010
		LT51290342010198IKR00	129/034	17/07/2010
		LT51290352010198IKR00	129/035	17/07/2010
		LT51300342010253IKR00	130/034	10/09/2010
2015	Landsat 8 Operational Land Imager and Thermal Infrared Sensor	LC81290332015244LGN00	129/033	01/09/2015
		LC81290342015244LGN00	129/034	01/09/2015
		LC81290352015196LGN00	129/035	15/07/2015
		LC81300342015187LGN00	130/034	06/07/2015

Aerospace Exploration Agency (JAXA); National Geomatics Center of China, 2014). Although GlobeLand30 was only released in 2014 it has been applied extensively at national and regional levels in various countries with high levels of accuracy (Brovelli et al., 2015; Jokar Arsanjani et al., 2016a; Jokar Arsanjani et al., 2016b; Manakos et al., 2014; Shi et al., 2016; Walker et al., 2010) and evaluation is ongoing. The GlobeLand30 is a Landsat-based product generated by the National Geomatics Center of China (NGCC) (J. Chen et al., 2015). This product represents the first attempt to create global land cover maps for the years 2000 and 2010 at 30 m resolution (J. Chen et al., 2015). The Japan Aerospace Exploration Agency (JAXA) produced the FNF data sets by classifying 25 m resolution satellite images into forest and non-forest areas. FNF data sets are available for the years 2007, 2008, 2009 and 2010 (Japan Aerospace Exploration Agency (JAXA) and Earth Observation Research Center (EORC)).

The ArcGIS software (ESRI, 2015) was used to generate random samples of training points from the GlobeLand30 and FNF data sets for the years 2000 and 2010. A total of approximately 500 training sites were selected for each year. In this way, it was possible to ensure that all land cover categories were adequately represented in the training statistics. Training data for these two years were not limited to the global land cover and FNF products. All the selected training points were cross-checked against historical imagery from Google Earth Pro (GEP) version 7.1.5.1557 (Google Inc., 2015). Google Earth archives display different forms of imagery obtained from multiple sources such as Landsat and QuickBird satellite sensors and various providers of digital photographs (Lemmens, 2011). GEP software is a widely-used platform for the collection of high resolution geo-referenced information on land cover, and also for the validation of land cover classification maps (Cha and Park, 2007; H. Chen et al., 2015; Q. Hu et al., 2013; Lu et al., 2015). GEP images from 2001, which is the earliest time point from which data are available for NHAR, and 2010 were used to evaluate the reference data. Training points that were located in indistinct areas in the GEP imagery or in areas that were covered by clouds were removed from the reference data sets.

The training data for 2000 and 2010 were also checked against GEP historical images from 2005 and 2015, respectively. Both, data sets and images were used to determine visually if land cover had changed between the periods 2000–2005 and 2010–2015. Training points from land areas that changed were discarded to locate and define training signatures for 2005 and 2015.

There were no historical records available for NHAR for the years 1991 and 1996 in GEP. Therefore, training data points for these years were derived from the reference data collected for 2000. Training sites from areas that were likely to remain unchanged based on previous visual interpretation of the GEP historical imagery were selected. In addition, the 1 km spatial resolution land use maps of China produced and provided by the Chinese Academy of Sciences for the 1980s, 1995 and 2000 served as supplementary information to define land cover features in the region.

For all images, visual interpretation of the Landsat data was also implemented to improve image classification. Visual comparisons of multiple sets of three spectral band combinations were conducted using ENVI software version 5.3 (Exelis Visual Information Solutions, 2015). This approach was used to better distinguish the different categories of the land cover scheme.

2.2.4. Reference data for validation

Reference validation data sets for accuracy assessment were created by collecting space- and time-referenced data uploaded to the website Panoramio (Google Inc.). The website is a photo-sharing service that contains geo-tagged photos from around the world. Web-based photo-sharing platforms, like Panoramio, are becoming an important data source with potential applications in multiple research contexts (Dong et al., 2014; Yu et al., 2014; Zhou et al., 2012).

Sets of photos for each year were downloaded and labelled manually based on visual interpretation and using the GlobeLand30 land cover classification scheme. Data were imported into ArcGIS to be projected to the same UTM zone used for the satellite images (ESRI, 2015). Reference points were buffered by 15 m to generate the training site polygons that were used to assess classification accuracy. Although most polygons were effective in distinguishing among different land cover types, the use of this type of data may introduce a level of uncertainty into the analyses (Fonte et al., 2015). Therefore, all polygons of each validation class were checked against historical satellite imagery from GEP. Reference data located in areas where land cover type was questionable were excluded from the analyses.

Although different data sources were used to create data sets for training and validation, from the total number of reference points selected, 425 (89.4%), 451 (90.0%), 486 (90.6%), 478 (90.5%), 500 (90.9%), 456 (90.1%) reference sites were used for training for the years 1996, 2001, 2005, 2010 and 2015, respectively. The reference data sets used for accuracy assessments included 50 polygons with approximately 2–3 pixels each.

2.3. Data analysis

2.3.1. Image classification

Pre-processing of the Landsat data was performed using the Landsat package (version 1.08) (Goslee, 2011) in the R language and environment for statistical computing (R Core Team, 2016). The Minnaert topographic correction method was applied independently to each spectral band to improve image comparability between dates. The spectral bands were stacked together and saved as a multiband image in TIFF format. To reduce the effects of clouds, cloud and cloud shadow removal were performed. The Landsat scenes for each date were mosaicked together and classified using ENVI version 5.3 (Exelis Visual Information Solutions, 2015). The maximum likelihood algorithm was the selected method for the process of supervised classification (Supplementary material Table A.1). Assuming a normal distribution of the data, this algorithm considers both the variance and covariance of class signatures to assign unknown pixels to a specific land cover class (Lillesand et al., 2014; Strahler, 1980).

The land cover classes were grouped into seven categories according to the spectral reflectance values and the objectives of the study. Because the reference data for classification was derived primarily from GlobeLand30, the classification scheme adopted was based on the land cover classification system established by the NGCC (Table 2).

Post-classification refinements were applied to reduce errors in the process of classification. Due to significant spectral confusion among the classes, artificial surfaces and bare or sparsely vegetated areas, these two classes were merged and represented as a single category in the maps and subsequent analyses.

Using the ENVI software, confusion matrices were calculated to assess the accuracy of the land cover classification maps. A confusion matrix is a simple cross-tabulation of each mapped class vs. the reference information (Foody, 2002; Lillesand et al., 2014). The overall accuracy of the classification, Kappa coefficient and user's and producer's accuracy were derived from the confusion matrices. The Kappa statistic reflects the difference between actual agreement between reference data and the classified maps and the agreement expected by chance. A Kappa value of 1 indicates perfect agreement, while a value of 0 indicates no agreement (Foody, 2002). User's accuracy provides an estimate of the probability that a pixel from the land cover map matches the same category in the reference data (it measures errors of commission), whereas the producer's accuracy estimates the probability that a reference pixel has been mapped correctly (it measures errors of omission) (Foody, 2002; Lillesand et al., 2014).

Table 2
Land cover classification scheme and definitions.

Land cover type	Description	Content
Water bodies	All areas of water	Streams and canals, lakes, reservoirs, bays and estuaries
Artificial surfaces	Land modified by human activities	Residential areas, industrial and commercial complexes, transport infrastructure, communications and utilities, mixed urban or built-up land and other built-up land
Bare or sparsely vegetated areas	Areas with little or no "green" vegetation present	Dry salt flats, sandy areas, bared exposed rock and mixed barren land
Herbaceous vegetation	Areas characterized by natural or semi-natural vegetation	Grasses and forbs
Cultivated land	Areas where the natural vegetation has been removed/modified and replaced by other types of vegetative cover that have been planted for specific purposes such as food, feed and gardening	Cropland and pasture, orchards, groves, vineyards, nurseries and ornamental horticultural, other cultivated land
Shrubland	Natural or semi-natural woody vegetation with aerial stems <6 m tall	Evergreen and deciduous species of true shrubs and trees or shrubs that are small or stunted
Forest	Areas characterized by tree cover or semi-natural woody vegetation >6 m tall	Deciduous forest, evergreen forest and mixed forest

2.3.2. Land cover change detection analysis

A post-classification change detection technique was performed using ENVI software (Exelis Visual Information Solutions, 2015). Cross-tabulation analyses were conducted to identify changes in land cover between 6 different time intervals 1991–1996, 1996–2000, 2000–2005, 2005–2010, 2010–2015 and 1991–2015. These tables indicate the number of pixels of a given class at time t_1 that are classified as the same or different class at time t_2 (from–to). This supports identification of changes in land cover as well as the identification of areas that have not changed.

3. Results

3.1. Land cover classification and change detection analysis

Confusion matrices showed that the overall classification accuracies were higher or equal to 80% and the total Kappa coefficients were >0.7. These results represent a substantial agreement between the reference data sets and the classified maps (Landis and Koch, 1977). The Kappa coefficients for 1991, 1996, 2000, 2005, 2010 and 2015 were 0.83, 0.83, 0.78, 0.72, 0.74 and 0.80, respectively. Most user's and producer's accuracies of individual classes were also generally high, ranging from 60% to 100% (Table 3).

Single date land cover maps were produced for each study year to show the spatial distribution of six land cover types in NHAR (Fig. 2). The geographic area covered by each individual class for all data products and the change statistics for 1991 and 2015, which were the temporal extremes of the project were calculated (Table 4 and Fig. 3).

From 1991 to 2015, herbaceous vegetation, cultivated land and forest increased by approximately 708,600 ha (12.2% of the study area), 164,300 ha (2.9%) and 410,200 ha (7.1%), respectively. Shrubland decreased by 22,000 ha (0.4%) and water decreased by 10,300 ha (0.2%). The largest relative change for the period 1991–2015 was observed in the area covered by forest, which increased by 273.1%. Forest expanded consistently in all periods, with the greatest increase occurring between 2010 and 2015. The change in forest was followed by the increase in herbaceous vegetation, 49.8%, and in cultivated land, 12.3%. Shrubland and water decreased, respectively, 66.7% and 22.2%. Although the extent of water and shrubland may have changed from year to year due to annual variability in precipitation and temperature, the minor changes observed in this category are likely to be partially explained by classification errors. Because artificial surfaces and bareland were merged into one a single class, it is difficult to interpret the changes observed in this land cover category over time.

To further evaluate the results of the different types of land cover conversions, cross-tabulation of the pair of maps 1991 and 1996, 1996 and 2000, 2005 and 2010, 2010 and 2015 were created (Table 5). In Table 5, the categories of the first map (vertical) are compared with those of the second map (horizontal) and tabulation is kept of the number of cells in each combination.

The results suggest that the area covered by herbaceous vegetation increased in all periods except in the interval 1996–2000 when it decreased by 88,900 ha. Although cultivated land increased over the whole study period, it experienced a decrease in the first five years of the study and between 2000 and 2010.

In 1991, forest, herbaceous vegetation and cultivated land covered an area of approximately 147,600 ha, 1,409,200 ha and 1,356,100 ha, respectively. In 2000, prior to the implementation of the GGP, the extent of land covered by these land cover types was 1,455,755 ha and 1,628,894 ha, respectively. By 2015, forest and herbaceous vegetation extended to 557,807 ha and 2,117,812 ha, while cultivated land was reduced to 1,520,435 ha.

The increase in forest resulted mainly from conversion of cultivated land and herbaceous vegetation in the twenty-five-year period. Of the 410,200 ha of total growth in forest between 1991 and 2015, 53.8% was converted from herbaceous vegetation and 30.8% from cultivated land. Although it is not possible to estimate the amount of land conversion, the increase in herbaceous vegetation came mainly from bareland and artificial surfaces.

The matrix created to show the land cover changes in NHAR during the whole study period (1990 to 2015) indicates that the decrease in water bodies (9300 ha) resulted mainly from conversion of cultivated land (Table 5f). This finding was also observed in the matrices developed for the 5-year periods. In NHAR, wetlands are mainly distributed in the irrigated plains of cultivated land. Therefore, the magnitude and location of the changes in the Yellow River Irrigated District suggest

Table 3
Summary of Landsat classification accuracies (%) for 1991, 1996, 2000, 2005, 2010 and 2015.

Land cover class	1991		1996		2000		2005		2010		2015	
	Producer's	User's	Producer's	User's	Producer's	User's	Producer's	User's	Producer's	User's	Producer's	User's
Bareland and artificial surfaces	100.0	85.7	100.0	60.1	66.6	100.0	84.4	84.4	89.2	60.1	100.0	82.6
Cultivated land	100.0	66.7	100.0	100.0	100.0	60.0	71.4	74.1	74.1	78.4	77.2	89.4
Herbaceous vegetation	66.6	100.0	60.0	100.0	100.0	60.1	66.7	69.7	75.0	85.7	80.0	92.3
Shrubland	100.0	80.0	100.0	100.0	100.0	100.0	–	–	–	–	–	–
Forest	–	–	–	–	–	–	66.6	60.2	80.0	88.8	100.0	61.5
Water	81.3	100.0	81.2	100.0	83.3	100.0	100.0	100.0	100.0	100.0	66.7	100
Overall accuracy	87.7		84.8		85.3		80.0		80.0		84.2	
Kappa statistic	0.8		0.7		0.7		0.7		0.7		0.8	

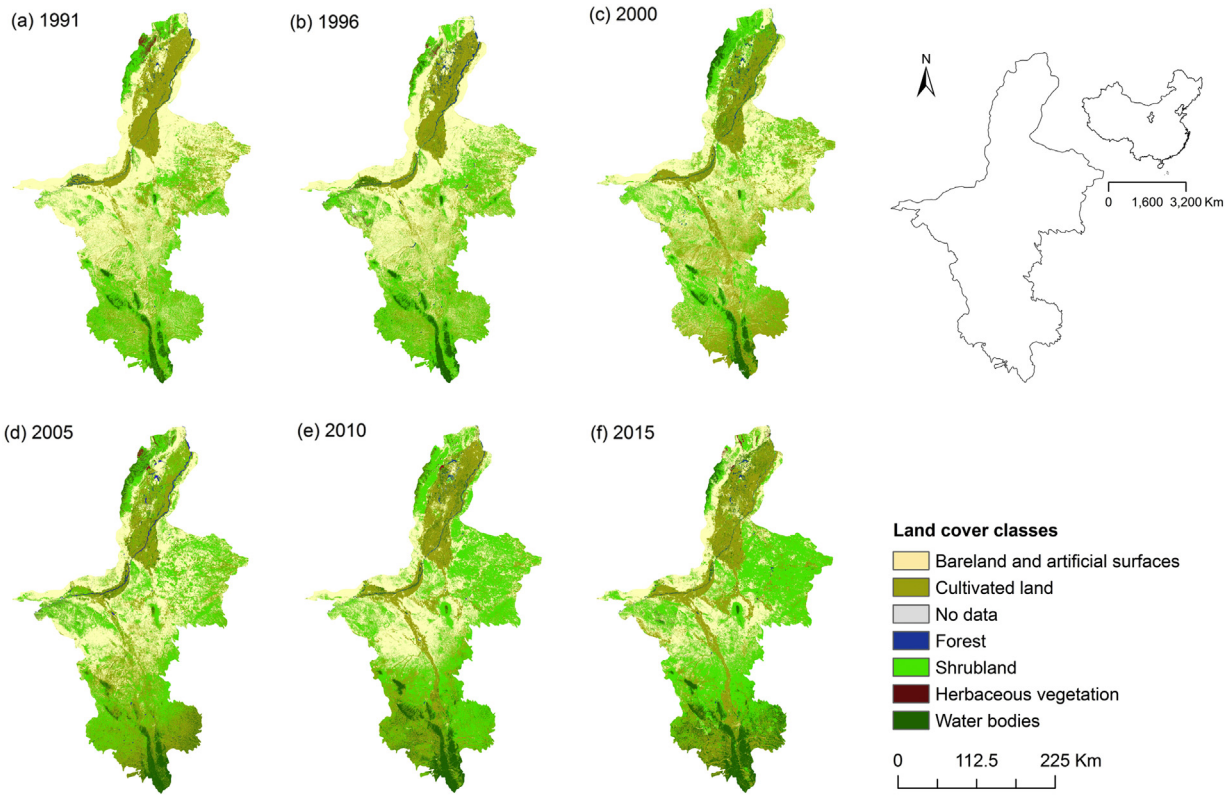

Fig. 2. Land cover classification maps for NHAR from (a) 1991, (b) 1996, (c) 2000, (d) 2005, (e) 2010, (f) 2015 and map of the location of the province in China.

that the results are most likely to be related to omission and commission errors in the Landsat classifications change map.

The changes in land cover that occurred in NHAR between 1991 and 2015 were not spatially homogeneous. The six land cover maps produced in the study reveal that land cover changes varied among the three different geographical regions. In general, the central desertified district and the southern mountainous and loess hilly district were the most transformed. Forest growth primarily occurred in the north and south of the province, in areas of the Helan and Liupan mountains in the north and south, respectively. The increase in herbaceous vegetation was mainly distributed in the central arid area of the province, and around the margin of forestland. Cultivated land dominated the landscape on the big plains of the northern Yellow River Irrigated District with a progressive linear expansion in the central area.

4. Discussion

The results of the present study are consistent with previous environmental assessments conducted in western China to describe the land cover changes that have occurred in regions where ecological restoration policies were adopted (Cao et al., 2009; Fan et al., 2015; Zhao et al., 2010). According to national estimates, by 2006, the GGP policy was responsible for the conversion of almost 9 million ha of cultivated land into forest and herbaceous vegetation, and the afforestation of 11.7 million ha of barren land (Liu et al., 2008). In the Loess Plateau, a region commonly characterized by drought, desertification and soil erosion, a rapid increase in vegetation cover was reported in the early 2000s after the implementation of the pilot phase of the program (Fan et al., 2015; Xin et al., 2008). The land cover changes observed in NHAR are in agreement with the key environmental goals of the GGP and previous short-term (ten years or less) land cover assessments conducted in the province using remote sensing or official national reports (Li et al., 2008; Qi et al., 2003; Wang et al., 2014; Zhang et al., 2008). In this study, forest, herbaceous vegetation and cultivated land coverages increased between 1991 and 2015. Similar findings were reported in other provinces such as Shaanxi located at the middle reaches of the Yellow River Basin (H. Chen et al., 2015), and Sichuan Province, located at the upper reaches of the Yangtze River (Yan-qiong et al., 2003). Reduction of surface runoff and soil erosion as a result of the implantation of the GGP in Hunan Province (2000–2005) was also reported (Li et al., 2006). However, these land cover changes were reported by researchers as positive or negative effects on the local environment based on the environmental needs of these regions.

As a consequence of rapid human population growth in NHAR, extensive areas of natural grassland were converted to cultivated land (Zhang et al., 2008). The overexploitation of land, together with

Table 4
Summary statistics of land cover maps from Ningxia Hui Autonomous Region by area (1000 ha).

Land cover class	1991 Area (%)	1996 Area (%)	2000 Area (%)	2005 Area (%)	2010 Area (%)	2015 Area (%)	Relative change 1991–2015 (%)
Water bodies	53.1 (0.9)	84.6 (1.5)	59.3 (1.0)	47.9 (0.8)	43.6 (0.8)	42.8 (0.7)	−22.2
Herbaceous vegetation	1409.2 (24.5)	1543.2 (26.8)	1455.7 (25.2)	1687.7 (29.3)	2022.3 (35.1)	2117.8 (36.7)	+49.8
Cultivated land	1356.1 (23.5)	1257.7 (21.9)	1628.8 (28.3)	1543.3 (26.8)	1504.4 (26.1)	1520.4 (26.4)	+12.3
Shrubland	35.4 (0.6)	27.0 (0.5)	0.3 (0.004)	33.9 (0.6)	7.8 (0.1)	13.4 (0.2)	−66.7
Forest	147.6 (2.6)	227.8 (4)	290.4 (5.1)	380.4 (6.6)	455.1 (7.9)	557.8 (9.7)	+273.1
Bareland and artificial surfaces	2757.9 (47.8)	2611.7 (45.4)	2321.9 (40.3)	2066.1 (35.9)	1726.1 (30)	1507.1 (26.2)	−45.2

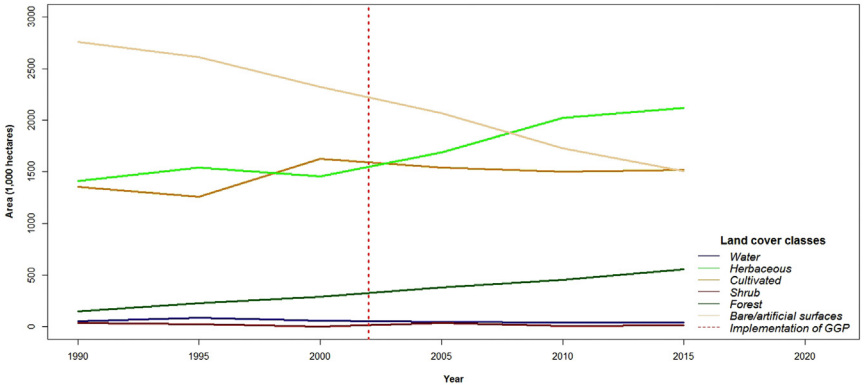

Fig. 3. Summary statistics of land cover maps from Ningxia Hui Autonomous Region by area (1000 ha).

intensive grazing of domestic animals contributed to the degradation of the local environment (Zhang et al., 2008). As part of the efforts to recover the landscape, including the implementation of the GGP, growth of artificial grass was promoted in the province while fencing natural grassland and applying grazing bans (Wang et al., 2014). Therefore, it may be possible that some of the policies implemented to improve ecological conditions may have led to the expansion of herbaceous vegetation and the more discrete increase in cultivated land.

The spatial variation in the distribution of the six land cover types and changes in NHAR between 1991 and 2015 can be explained partially by the contrasting climatic and topographic characteristics of the three geographical regions of the province. However, there are also other local environmental and socio-economic factors that may influence the local land use practices and lead to land cover change. NHAR is vulnerable to numerous meteorological hazards that have the potential to damage the land surface (Li et al., 2013). Drought, floods, torrential rain and high and low temperature stresses are particularly frequent in the region (Li et al., 2013). Between 2004 and 2006, a severe drought affected the region causing an important reduction in the availability of water for industrial and agricultural purposes (Li et al., 2013; Yang et al., 2015). This meteorological event had important environmental and economic consequences for the province, some of which were evident in this study. Decreases of 126,200 ha of cultivated land and 15,800 ha of water were observed between 2000 and 2010, particularly in the northern and the central part of the province, where irrigation water is mainly diverted from the Yellow River. These findings are in agreement with those mentioned previously in a report that promotes better adaptation strategies to minimise the effects of future environmental hazards (Yang et al., 2015).

NHAR is currently undergoing economic transition processes that also affect the use of land directly and indirectly (Wang et al., 2011). Land conversion is linked directly to socioeconomic development due to the effects of economic growth on urban expansion and exploitation of natural resources (Wang et al., 2011). Economic growth also influences positively the spatial structure of land use patterns by improving income opportunities from non-agricultural sectors, causing income diversification and promoting rural-urban migration (Peng, 2011). Population growth in NHAR has also been a dominant factor driving urban development processes, particularly in the north (Wu, 2002). Consequently, some cultivated land has been transformed rapidly into rural and urban built-up areas such as cities, roads, factories and mining infrastructure in past decades (Wu, 2002). Therefore, it is reasonable to conclude that most of the decrease in land area covered by the merged land cover class "bare or sparsely vegetated areas" and "artificial surfaces" corresponded to a reduction in bare and sparely vegetated areas. In the present study important changes in land cover were identified in NHAR between 1991 and 2015. These findings raise the need for further studies to determine the association of the GGP and other potential drivers of land cover change with the observed increases in forest cover, herbaceous vegetation and cultivated land. While current evidence recognises the role of national ecological rehabilitation projects in China, there is still a need for more holistic and rational approaches that examine the contributions of other economic and social factors in the process of landscape restoration in the country.

Ecological restoration policies, if implemented appropriately, can be effective measures to address pressing environmental concerns (Liu et al., 2008; Melillo et al., 2016; Nepstad et al., 2014). However, the mixture of natural and artificially modified landscapes has also important implications for the structure and function of ecosystems and human health. Environmental change has the potential to compromise food security by influencing food availability, accessibility, utilization and systems stability (Ingram et al., 2012). In addition, alterations to the climate and landscape features have been increasingly associated with variations in human disease patterns. This is particularly important for infectious diseases, where environmental change impacts on the geographic range of various mosquito-borne diseases such as malaria, dengue and leishmaniasis (Caminade et al., 2014; Colón-González et al., 2013; González et al., 2014) and non-mosquito-borne helminth infections, such as schistosomiasis and echinococcosis (Giraudoux et al., 2013; Gomes et al., 2012; Y. Hu et al., 2013). Quality evaluated land cover maps derived from remote sensing are important for such studies (Danson et al., 2004; Hamm et al., 2015; Navas et al., 2016; Pleydell et al., 2008). In hyper-endemic areas for echinococcosis in western China the geographical patterns of alveolar echinococcosis infection have been associated with the recent implementation of land reform policies in the region (Giraudoux et al., 2013; Pleydell et al., 2008). Land cover transformations that result from land reforms are likely to alter the transmission of *Echinococcus* spp. by influencing human behaviour, animal population dynamics, spatial and temporal overlap of intermediate and definitive hosts and the survival of the parasite eggs in the external environment (Cadavid Restrepo et al., 2015). Further studies may need to be conducted to test the association between land cover change and infection patterns of human echinococcosis.

Although some effects of global environmental change can be anticipated, most of the impacts depend on local vulnerabilities and the implementation of effective strategies for adaptation (McCarthy, 2001). Accurate predictions of LULC can only be estimated when there is an adequate availability of local socio-economic and baseline data (Lambin and Geist, 2008). This study allowed us to identify spatial and temporal patterns in land cover change trends in NHAR in the last 30 years. The findings provide accurate information, in space and time, and visual representations of the areas that are most affected by land cover change. Therefore, these results are a reasonable starting point from which to conduct future research in NHAR to explore, monitor and predict future environmental change and its short- and long-term effects on the well-being of the population.

The main challenges of the study include the limited availability of historical satellite and reference data to train the classifier and validate

Table 5
Matrices of land cover changes (1000 ha) from 1991 to 2015.

a. Period 1991–1996

1996	1991						1996 total
	Water bodies	Herbaceous vegetation	Cultivated land	Shrubland	Forest	Bareland/artificial surfaces	
Water bodies	40.0	3.1	33.8	0.3	0.1	7.0	84.3
Herbaceous vegetation	0.8	1104.5	211.6	17.5	10.8	198.0	1542.0
Cultivated land	6.7	92.5	1024.5	0.6	5.1	128.2	1257.6
Shrubland	0.2	10.5	0.4	10.1	0.0	5.7	27.0
Forest	3.8	54.1	35.8	1.7	131.0	0.6	227.0
Bareland and artificial surfaces	0.8	142.7	49.9	5.1	0.1	2411.9	2610.5
Difference	32.0	134.6	−98.4	−8.4	80.0	−140.9	
1991 total	52.3	1407.4	1356.0	35.4	147.0	2751.4	5748.0

b. Period 1996–2000

2000	1996						2000 total
	Water bodies	Herbaceous vegetation	Cultivated land	Shrubland	Forest	Bareland/artificial surfaces	
Water bodies	33.6	2.4	15.2	0.4	1.7	5.8	59.3
Herbaceous vegetation	18.6	634.7	226.9	15.5	44.4	513.1	1453.1
Cultivated land	21.1	387.3	685.5	0.2	43.6	490.8	1628.4
Shrubland	0.0	0.1	0.0	0.1	0.0	0.1	0.3
Forest	3.7	59.8	77.1	5.3	133.6	10.9	290.3
Bareland and artificial surfaces	7.5	457.8	252.8	5.5	3.7	1589.7	2317.1
Difference	−25.2	−88.9	370.8	−26.7	63.3	−293.3	
1996 total	84.5	1542.0	1257.6	27.0	227.0	2610.4	5748.0

c. Period 2000–2005

2005	2000						2005 total
	Water bodies	Herbaceous vegetation	Cultivated land	Shrubland	Forest	Bareland/artificial surfaces	
Water bodies	27.5	8.1	5.7	0.0	2.2	4.0	47.5
Herbaceous vegetation	10.3	687.5	373.8	0.1	47.7	566.0	1685.4
Cultivated land	7.8	326.1	786.9	0.005	83.3	338.0	1542.1
Shrubland	1.0	17.9	1.7	0.1	9.9	3.2	33.8
Forest	5.8	82.8	133.3	0.0	139.6	17.5	379.0
Bareland and artificial surfaces	6.9	330.0	327.0	0.0	7.5	1389.0	2060.4
Difference	−11.8	233.0	−88.3	33.6	88.8	−257.3	
2000 total	59.3	1452.4	1628.4	0.2	290.2	2317.7	5748.0

d. Period 2005–2010

2010	2005						2010 total
	Water bodies	Herbaceous vegetation	Cultivated land	Shrubland	Forest	Bareland/artificial surfaces	
Water bodies	25.5	5.3	5.4	0.1	1.7	5.5	43.5
Herbaceous vegetation	2.1	922.0	460.8	21.8	72.9	542.7	2022.3
Cultivated land	9.9	386.1	753.8	2.1	95.5	257.2	1504.6
Shrubland	0.2	1.4	0.2	3.4	0.7	1.8	7.7
Forest	3.8	82.2	168.3	1.0	193.0	6.8	455.1
Bareland and artificial surfaces	6.0	289.0	154.0	5.5	15.0	1245.0	1714.5
Difference	−4.0	1100.3	−37.9	−26.2	76.1	−345.5	
2005 total	47.5	1686.0	1542.5	33.9	379.0	2060.0	5748.0

e. Period 2010–2015

2015	2010 Total						2015 total
	Water bodies	Herbaceous vegetation	Cultivated land	Shrubland	Forest	Bareland/artificial surfaces	
Water bodies	26.8	1.4	5.6	0.3	3.1	5.5	42.8
Herbaceous vegetation	1.0	1294.2	276.6	0.4	45.7	500.0	2117.2
Cultivated land	10.8	235.5	963.9	0.2	129.5	180.0	1519.0
Shrubland	0.0	6.7	0.3	2.8	0.3	3.3	13.4
Forest	0.8	123.9	152.4	1.2	271.0	8.4	557.7
Bareland and artificial surfaces	3.9	360.5	105.5	2.9	5.6	1017.5	1496.0
Difference	−0.6	95.2	15.0	5.6	102.5	−218.7	
2010 total	43.4	2022.0	1504.3	7.8	455.2	1714.7	5748.0

f. Period 1991–2015

2015	1991						2015 total
	Water bodies	Herbaceous vegetation	Cultivated land	Shrubland	Forest	Bareland/artificial surfaces	
Water bodies	15.9	2.9	14.7	0.1	0.3	8.9	42.8
Herbaceous vegetation	2.4	689.4	307.0	12.5	9.9	1096.0	2117.2

Table 5 (*continued*)

f. Period 1991–2015

2015	1991						2015 total
	Water bodies	Herbaceous vegetation	Cultivated land	Shrubland	Forest	Bareland/artificial surfaces	
Cultivated land	27.5	279.9	724.6	1.7	16.1	470.0	1519.8
Shrubland	0.1	5.2	0.6	2.4	0.01	5.1	13.4
Forest	2.8	230.5	142.5	1.9	120.7	59.3	557.7
Bareland and artificial surfaces	3.4	199.0	166.7	16.7	0.6	1110.4	1496.8
Difference	−9.3	710.2	163.7	−22.0	410.1	−1253.2	
1991 total	52.1	1407.0	1356.1	35.4	147.6	2750.0	5748.0

the land cover maps. When analysing time-series data sets, quality and consistency in the data are essential to identify the real changes that occur in the environment (Hamm et al., 2015; Stehman, 2009). In this study, part of the disagreement between the Landsat scenes and the reference training data sets may be attributed to the fact that there were no images for the specified period in some locations. For some years it was necessary to derive data from different growing seasons. In addition, the use of Globeland30 and the FNF maps may have introduced some uncertainty into the analysis because they are also land cover products that may contain classification errors that by default were included in the analyses. Although the reference training data obtained from these maps allowed us to classify the satellite images with good accuracy, a more traditional approach that incorporates different data sources and a combination of field studies would be preferred (Stehman, 2009). The land cover classification scheme used in the study was derived from the land cover classification system established by the NGCC. Although the use of this legend allowed comparability between land cover datasets, the interpretation of the land cover changes found in the study with respect to the GGP goals also represented a challenge (Fritz and See, 2008; Tchuenté et al., 2011). Based on similarities of definitions, the changes found in herbaceous vegetation and cultivated land were compared to the project goals with respect to grasslands and croplands, respectively.

5. Conclusions

The present study explores and quantifies the changes in land cover that occurred in NHAR during a period of extensive landscape regeneration. The results of the analysis of land cover change conducted in this study concur with the large-scale impact of the GGP in increasing forest and herbaceous vegetation coverage and in regenerating bareland area. These results provide evidence that may help facilitate future landscape planning, management and decision making in the province. In addition, this assessment of land cover change may help to explain and respond effectively to emerging environmental risks in NHAR.

Supplementary data to this article can be found online at http://dx.doi.org/10.1016/j.scitotenv.2017.04.124.

Acknowledgements

The authors are grateful to the Chinese Academy of Sciences for providing us with the climate data from 1980 to 2013. We acknowledge financial support by the National Health and Medical Research Council (NHMRC) of Australia of a NHMRC Project Grant (APP1009539). AMCR is a PhD Candidate supported by a Postgraduate Award from The Australian National University; ACAC is a NHMRC Senior Research Fellow; DPM is a NHMRC Senior Principal Research Fellow; and DJG is a NHMRC Career Development Fellow. The funders had no role in study design, data collection and analysis, decision to publish, or preparation of the manuscript.

References

Blaikie, P., Brookfield, H., 2015. Land Degradation and Society. Routledge.
Bommarco, R., Kleijn, D., Potts, S.G., 2013. Ecological intensification: harnessing ecosystem services for food security. Trends Ecol. Evol. 28, 230–238.
Broich, M., Huete, A., Tulbure, M., Ma, X., Xin, Q., Paget, M., et al., 2014. Land surface phenological response to decadal climate variability across Australia using satellite remote sensing. Biogeosciences 11, 5181–5198.
Brovelli, M.A., Molinari, M.E., Hussein, E., Chen, J., Li, R., 2015. The first comprehensive accuracy assessment of GlobeLand30 at a national level: methodology and results. Remote Sens. 7, 4191–4212.
Cadavid Restrepo, A.M., Yang, Y., McManus, D., Gray, D., Giraudoux, P., Barnes, T., et al., 2015. The landscape epidemiology of echinococcoses. Infect. Dis. Poverty 5, 13.
Caminade, C., Kovats, S., Rocklov, J., Tompkins, A.M., Morse, A.P., Colón-González, F.J., et al., 2014. Impact of climate change on global malaria distribution. Proc. Natl. Acad. Sci. 111, 3286–3291.
Cao, S., Chen, L., Yu, X., 2009. Impact of China's Grain for Green Project on the landscape of vulnerable arid and semi-arid agricultural regions: a case study in northern Shaanxi Province. J. Appl. Ecol. 46, 536–543.
Carpenter, S.R., DeFries, R., Dietz, T., Mooney, H.A., Polasky, S., Reid, W.V., et al., 2006. Millennium ecosystem assessment: research needs. Science 314, 257–258.
Carreiras, J.M., Jones, J., Lucas, R.M., Gabriel, C., 2014. Land use and land cover change dynamics across the Brazilian Amazon: insights from extensive time-series analysis of remote sensing data. PLoS One 9, e104144.
Cha, S.-y., Park, C.-H., 2007. The utilization of Google Earth images as reference data for the multitemporal land cover classification with MODIS data of North Korea. Kor. J. Remote Sens. 23, 483–491.
Chen, H., Marter-Kenyon, J., López-Carr, D., Liang, X.-y., 2015a. Land cover and landscape changes in Shaanxi Province during China's Grain for Green Program (2000−2010). Environ. Monit. Assess. 187, 1–14.
Chen, J., Chen, J., Liao, A., Cao, X., Chen, L., Chen, X., et al., 2015b. Global land cover mapping at 30 m resolution: a POK-based operational approach. ISPRS J. Photogramm. Remote Sens. 103, 7–27.
Colón-González, F.J., Fezzi, C., Lake, I.R., Hunter, P.R., 2013. The effects of weather and climate change on dengue. PLoS Negl. Trop. Dis. 7, e2503.
Danson, F.M., Craig, P.S., Man, W., Shi, D., Giraudoux, P., 2004. Landscape dynamics and risk modeling of human alveolar echinococcosis. Photogramm. Eng. Remote. Sens. 70, 359–366.
Department of the Interior - The United States Geological Survey (USGS), 2016a. Landsat 4–7 Climate Data Record (CDR) Surface Reflectance, Version 6.4. product guide. http://landsat.usgs.gov/documents/cdr_sr_product_guide.pdf (accessed 2 May 2016).
Department of the Interior - The United States Geological Survey (USGS), 2016b. Provisional Landsat 8 Surface Reflectance Product. http://landsat.usgs.gov/documents/provisional_l8sr_product_guide.pdf (accessed 2 May 2016).
Dong, J., Xiao, X., Sheldon, S., Biradar, C., Zhang, G., Duong, N.D., et al., 2014. A 50-m forest cover map in Southeast Asia from ALOS/PALSAR and its application on forest fragmentation assessment. PLoS One 9, e85801.
ESRI. Environmental Systems Research Institute. ArcGIS Software version 10.3.1. Redlands. California, 2015.
Exelis Visual Information Solutions I. ENVI software version 5.3. Boulder, CO, USA. 2015.
Fan, X., Ma, Z., Yang, Q., Han, Y., Mahmood, R., Zheng, Z., 2015. Land use/land cover changes and regional climate over the Loess Plateau during 2001–2009. Part I: observational evidence. Clim. Chang. 129, 427–440.
Foley, J.A., DeFries, R., Asner, G.P., Barford, C., Bonan, G., Carpenter, S.R., et al., 2005. Global consequences of land use. Science 309, 570–574.
Fonte, C.C., Bastin, L., See, L., Foody, G., Lupia, F., 2015. Usability of VGI for validation of land cover maps. Int. J. Geogr. Inf. Sci. 29, 1269–1291.
Foody, G.M., 2002. Status of land cover classification accuracy assessment. Remote Sens. Environ. 80, 185–201.
Fritz, S., See, L., 2008. Identifying and quantifying uncertainty and spatial disagreement in the comparison of Global Land Cover for different applications. Glob. Chang. Biol. 14, 1057–1075.
Giraudoux, P., Raoul, F., Pleydell, D., Li, T., Han, X., Qiu, J., et al., 2013. Drivers of Echinococcus multilocularis transmission in China: small mammal diversity, landscape or climate? PLoS Negl. Trop. Dis. 7, e2045.
Gomes, E., Leal-Neto, O.B., Albuquerque, J., da Silva, H., Barbosa, C.S., 2012. Schistosomiasis transmission and environmental change: a spatio-temporal analysis in Porto de Galinhas, Pernambuco-Brazil. Int. J. Health Geogr. 11, 51.
González, C., Paz, A., Ferro, C., 2014. Predicted altitudinal shifts and reduced spatial distribution of Leishmania infantum vector species under climate change scenarios in Colombia. Acta Trop. 129, 83–90.
Google Inc., 2015. Google Earth Pro version 7.1.5.1557. https://www.google.com.au/earth/ (accessed 25 January 2016).
Google Inc., 2016. Panoramio. Photos of the world. http://www.panoramio.com/ (accessed 16 February 2016, 16 February).

Goslee, S.C., 2011. Analyzing remote sensing data in R: the landsat package. J. Stat. Softw. 43, 1–25.
Hamm, N.A.S., Soares Magalhães, R.J., Clements, A.C.A., 2015. Earth observation, spatial data quality, and neglected tropical diseases. PLoS Negl. Trop. Dis. 9, e0004164.
Hu, Q., Wu, W., Xia, T., Yu, Q., Yang, P., Li, Z., et al., 2013a. Exploring the use of Google Earth imagery and object-based methods in land use/cover mapping. Remote Sens. 5, 6026–6042.
Hu, Y., Zhang, Z., Chen, Y., Wang, Z., Gao, J., Tao, B., et al., 2013b. Spatial pattern of schistosomiasis in Xingzi, Jiangxi Province, China: the effects of environmental factors. vectors]–>Parasit. Vectors 6, 1.
Ingram, J., Ericksen, P., Liverman, D., 2012. Food Security and Global Environmental Change. Earthscan, London, UK.
Japan Aerospace Exploration Agency (JAXA), d. Global 25m Resolution PALSAR-2/PALSAR Mosaic and Forest/Non-Forest Maphttp://www.eorc.jaxa.jp/ALOS/en/palsar_fnf/data/index.htm (accessed 25 February 2016).
Japan Aerospace Exploration Agency (JAXA), Earth Observation Research Center (EORC), d. Global 25m Resolution PALSAR-2/PALSAR Mosaic and Forest/Non-Forest Map (FNF). Dataset descriptionhttp://www.eorc.jaxa.jp/ALOS/en/palsar_fnf/DatasetDescription_PALSAR2_Mosaic_FNF_revA.pdf (accessed 25 February 2016).
Jokar Arsanjani, J., See, L., Tayyebi, A., 2016a. Assessing the suitability of GlobeLand30 for mapping land cover in Germany. Int. J. Digital Earth 1–19.
Jokar Arsanjani, J., Tayyebi, A., Vaz, E., 2016b. GlobeLand30 as an alternative fine-scale global land cover map: challenges, possibilities, and implications for developing countries. Habitat Int. 55, 25–31.
Kalnay, E., Cai, M., 2003. Impact of urbanization and land-use change on climate. Nature 423, 528–531.
Lambin, E.F., Geist, H.J., 2008. Land-use and Land-cover Change: Local Processes and Global Impacts. Springer Science & Business Media.
Lambin, E.F., Turner, B.L., Geist, H.J., Agbola, S.B., Angelsen, A., Bruce, J.W., et al., 2001. The causes of land-use and land-cover change: moving beyond the myths. Glob. Environ. Chang. 11, 261–269.
Landis, J.R., Koch, G.G., 1977. The measurement of observer agreement for categorical data. Biometrics 33, 159–174.
Lemmens, M., 2011. Geo-information: Technologies, Applications and the Environment. vol. 5. Springer Science & Business Media.
Li, D., Bo, F., Tao, J., 2006. Achievements in and strategies for Grain to Green Program in Hunan Province. Hunan For. Sci. Technol. 33, 1–5.
Li, J., Zheng, G., Liu, H., Wang, L., Tang, Z., Shi, H., et al., 2008. Situation Analysis of Ningxia Province. China Climate Change Partnership Framework - Enhanced Strategies for Climate-proofed and Environmentally Sound Agricultural Production in the Yellow River Basin (C-PESAP).
Li, Y., Conway, D., Wu, Y., Gao, Q., Rothausen, S., Xiong, W., et al., 2013. Rural livelihoods and climate variability in Ningxia, Northwest China. Clim. Chang. 119, 891–904.
Lillesand, T., Kiefer, R.W., Chipman, J., 2014. Remote Sensing and Image Interpretation. John Wiley & Sons.
Liu, J., Diamond, J., 2005. China's environment in a globalizing world. Nature 435, 1179–1186.
Liu, J., Li, S., Ouyang, Z., Tam, C., Chen, X., 2008. Ecological and socioeconomic effects of China's policies for ecosystem services. Proc. Natl. Acad. Sci. 105, 9477–9482.
Liu, J., Kuang, W., Zhang, Z., Xu, X., Qin, Y., Ning, J., et al., 2014. Spatiotemporal characteristics, patterns, and causes of land-use changes in China since the late 1980s. J. Geogr. Sci. 24, 195–210.
Lu, N., Hernandez, A.J., Ramsey, R.D., 2015. Land cover dynamics monitoring with Landsat data in Kunming, China: a cost-effective sampling and modelling scheme using Google Earth imagery and random forests. Geocarto Int. 30, 186–201.
Manakos, I., Chatzopoulos-Vouzoglanis, K., Petrou, Z.I., Filchev, L., Apostolakis, A., 2014. Globalland30 mapping capacity of land surface water in Thessaly, Greece. Land 4, 1–18.
McCarthy, J.J., 2001. Climate Change 2001: Impacts, Adaptation, and Vulnerability: Contribution of Working Group II to the Third Assessment Report of the Intergovernmental Panel on Climate Change. Cambridge University Press.
Melillo, J.M., Lu, X., Kicklighter, D.W., Reilly, J.M., Cai, Y., Sokolov, A.P., 2016. Protected areas' role in climate-change mitigation. Ambio 45, 133–145.
National Bureau of Statistics of China, 2014. China Statistical Year Book 2014. Population and its composition. http://www.stats.gov.cn/tjsj/ndsj/2014/indexeh.htm (accessed 2 June 2016).
National Geomatics Center of China, 2014. GlobeLand30. A 30-meter Global Land Cover Dataset. http://glc30.tianditu.com/ (accessed 12 December 2015).
Navas, A.L.A., Hamm, N.A.S., Magalhães, R.J.S., Stein, A., 2016. Mapping soil transmitted helminths and schistosomiasis under uncertainty: a systematic review and critical appraisal of evidence. PLoS Negl. Trop. Dis. 10, e0005208.
Nepstad, D., McGrath, D., Stickler, C., Alencar, A., Azevedo, A., Swette, B., et al., 2014. Slowing Amazon deforestation through public policy and interventions in beef and soy supply chains. Science 344, 1118.
Newbold, T., Hudson, L.N., Hill, S.L., Contu, S., Lysenko, I., Senior, R.A., et al., 2015. Global effects of land use on local terrestrial biodiversity. Nature 520, 45–50.
de Noblet-Ducoudré, N., Boisier, J.-P., Pitman, A., Bonan, G., Brovkin, V., Cruz, F., et al., 2012. Determining robust impacts of land-use-induced land cover changes on surface climate over North America and Eurasia: results from the first set of LUCID experiments. J. Clim. 25, 3261–3281.
Peng, X., 2011. China's demographic history and future challenges. Science 333, 581–587.
Pielke, R.A., 2005. Land use and climate change. Science 310, 1625–1626.
Pielke, R.A., Marland, G., Betts, R.A., Chase, T.N., Eastman, J.L., Niles, J.O., et al., 2002. The influence of land-use change and landscape dynamics on the climate system: relevance to climate-change policy beyond the radiative effect of greenhouse gases. Philos. Trans. R. Soc. A Math. Phys. Eng. Sci. 360, 1705–1719.
Pleydell, D.R., Yang, Y.R., Danson, F.M., Raoul, F., Craig, P.S., McManus, D.P., et al., 2008. Landscape composition and spatial prediction of alveolar echinococcosis in southern Ningxia, China. PLoS Negl. Trop. Dis. 2, e287.
Qi, Y., Wang, Y., Wang, J., 2003. Ningxia land cover change and its driving factors during past decade. Third International Asia-Pacific Environmental Remote Sensing Remote Sensing of the Atmosphere, Ocean, Environment, and Space. International Society for Optics and Photonics, pp. 844–853.
R Core Team, 2016. R: A Language and Environment for Statistical Computing. R Foundation for Statistical Computing, Vienna, Austria URL. https://www.R-project.org.
Raj, R., Hamm, N.A.S., Kant, Y., 2013. Analysing the effect of different aggregation approaches on remotely sensed data. Int. J. Remote Sens. 34, 4900–4916.
Sala, O.E., Chapin, F.S., Armesto, J.J., Berlow, E., Bloomfield, J., Dirzo, R., et al., 2000. Global biodiversity scenarios for the year 2100. Science 287, 1770–1774.
Sawaya, K.E., Olmanson, L.G., Heinert, N.J., Brezonik, P.L., Bauer, M.E., 2003. Extending satellite remote sensing to local scales: land and water resource monitoring using high-resolution imagery. Remote Sens. Environ. 88, 144–156.
Shalaby, A., Tateishi, R., 2007. Remote sensing and GIS for mapping and monitoring land cover and land-use changes in the Northwestern coastal zone of Egypt. Appl. Geogr. 27, 28–41.
Shi, X., Nie, S., Ju, W., Yu, L., 2016. Application and impacts of the GlobeLand30 land cover dataset on the Beijing Climate Center Climate Model. IOP Conference Series: Earth and Environmental Science vol. 34, p. 012032.
Statistical Bureau of Ningxia Hui Autonomous Region, 2014. Population Ningxia 2014. http://www.nxtj.gov.cn/nxtjjxbww/tjxx/201503/t20150310_52808.html (accessed 20 March 2016).
Stehman, S.V., 2009. Sampling designs for accuracy assessment of land cover. Int. J. Remote Sens. 30, 5243–5272.
Strahler, A.H., 1980. The use of prior probabilities in maximum likelihood classification of remotely sensed data. Remote Sens. Environ. 10, 135–163.
Tchuenté, A.T.K., Roujean, J.-L., De Jong, S.M., 2011. Comparison and relative quality assessment of the GLC2000, GLOBCOVER, MODIS and ECOCLIMAP land cover data sets at the African continental scale. Int. J. Appl. Earth Obs. Geoinf. 13, 207–219.
The National Aeronautics and Space Administration (NASA), Ministry of Economy Trade and Industry (METI), 2011. The Advanced Spaceborne Thermal Emission and Reflection Radiometer (ASTER) Global Digital Elevation Model (GDEM). Version 2. ASTER GDEM is a product of NASA and METI. https://asterweb.jpl.nasa.gov/gdem.asp (accessed 16 November 2015).
The United States Geological Survey (USGS), d. EarthExplorerhttp://earthexplorer.usgs.gov/ (accessed 14 June 2015).
The University of Nottingham, 2010. China Policy Institute. "Grain for Green Programme". China: Policy Making and Implementation? Briefing Series (Issue 60).
Turner, I., Moss, R., Sz Skole, D., 1993. Relating Land Use and Global Land-cover Change: A Proposal for an IGBP–HDP Core Project. Report From the IGBP-HDP Working Group on Land Use/Land-cover Change. Joint Publication of the International Geosphere-Biosphere Programme (Report No. 24) and the Human Dimensions of Global Environmental Change Programme (Report No. 5). Royal Swedish Academy of Science, Stockholm.
Turner, B.L., Lambin, E.F., Reenberg, A., 2007. The emergence of land change science for global environmental change and sustainability. Proc. Natl. Acad. Sci. 104, 20666–20671.
Verburg, P.H., van de Steeg, J., Veldkamp, A., Willemen, L., 2009. From land cover change to land function dynamics: a major challenge to improve land characterization. J. Environ. Manag. 90, 1327–1335.
Vitousek, P.M., Mooney, H.A., Lubchenco, J., Melillo, J.M., 1997. Human domination of Earth's ecosystems. Science 277, 494–499.
Walker, W.S., Stickler, C.M., Kellndorfer, J.M., Kirsch, K.M., Nepstad, D.C., 2010. Large-area classification and mapping of forest and land cover in the Brazilian Amazon: a comparative analysis of ALOS/PALSAR and Landsat data sources. IEEE J. Sel. Top. Appl. Earth Obs. Remote Sens. 3, 594–604.
Wang, X., Lu, C., Fang, J., Shen, Y., 2007. Implications for development of grain-for-green policy based on cropland suitability evaluation in desertification-affected north China. Land Use Policy 24, 417–424.
Wang, C., Yang, Y., Zhang, Y., 2011. Economic development, rural livelihoods, and ecological restoration: evidence from China. Ambio 40, 78–87.
Wang, Y., Gao, J., Wang, J., Qiu, J., 2014. Value assessment of ecosystem services in nature reserves in Ningxia, China: a response to ecological restoration. PLoS One 9, e89174.
Weng, Q., 2002. Land use change analysis in the Zhujiang Delta of China using satellite remote sensing, GIS and stochastic modelling. J. Environ. Manag. 64, 273–284.
Wu, W., 2002. Land use and cover change detection and modelling for North Ningxia, China. Proceedings of Map Asia 2002. GIS Development Webpage. http://www.gisdevelopment.net/application/environment/overview/envo0008pf.htm.
Xin, Z., Xu, J., Zheng, W., 2008. Spatiotemporal variations of vegetation cover on the Chinese Loess Plateau (1981–2006): impacts of climate changes and human activities. China Series D: Earth Sciences]–>Sci. China Ser. D Earth Sci. 51, 67–78.
Xu, X., Tan, Y., Yang, G., 2013. Environmental impact assessments of the Three Gorges Project in China: issues and interventions. Earth Sci. Rev. 124, 115–125.
Yang, J., Tan, C., Wang, S., Wang, S., Yang, Y., Chen, H., 2015. Drought adaptation in the Ningxia Hui Autonomous Region, China: actions, planning, pathways and barriers. Sustainability 7, 15029–15056.
Yan-qiong, Y., Guo-jie, C., Hong, F., 2003. Impacts of the "Grain for Green" project on rural communities in the Upper Min River Basin, Sichuan, China. Mt. Res. Dev. 23, 345–352.

Yin, R., Yin, G., 2010. China's primary programs of terrestrial ecosystem restoration: initiation, implementation, and challenges. Environ. Manag. 45, 429–441.
Yu, L., Wang, J., Li, X., Li, C., Zhao, Y., Gong, P., 2014. A multi-resolution global land cover dataset through multisource data aggregation. China Earth Sciences]–>Sci. China Earth Sci. 57, 2317–2329.
Yuan, F., Sawaya, K.E., Loeffelholz, B.C., Bauer, M.E., 2005. Land cover classification and change analysis of the Twin Cities (Minnesota) Metropolitan Area by multitemporal Landsat remote sensing. Remote Sens. Environ. 98, 317–328.
Zhang, L., Tu, Q., Mol, A.P., 2008. Payment for environmental services: the sloping land conversion program in Ningxia autonomous region of China. Chin. World. Econ. 16, 66–81.
Zhao, X., Lv, X., Dai, J., 2010. Impact assessment of the "Grain for Green Project" and discussion on the development models in the mountain-gorge regions. Front. Earth Sci. China 4, 105–116.
Zhou, D., Zhao, S., Zhu, C., 2012. The Grain for Green Project induced land cover change in the Loess Plateau: a case study with Ansai County, Shanxi Province, China. Ecol. Indic. 23, 88–94.